Original Article

MOLECULAR METABOLISM

The gut hormone receptor GIPR links energy availability to the control of hematopoiesis

Gemma Pujadas, Elodie M. Varin, Laurie L. Baggio, Erin E. Mulvihill [1], K.W.Annie Bang, Jacqueline A. Koehler, Dianne Matthews, Daniel J. Drucker*

ABSTRACT

Objective: Glucose-dependent insulinotropic polypeptide (GIP) conveys information from ingested nutrients to peripheral tissues, signaling energy availability. The GIP Receptor (GIPR) is also expressed in the bone marrow, notably in cells of the myeloid lineage. However, the importance of gain and loss of GIPR signaling for diverse hematopoietic responses remains unclear.

Methods: We assessed the expression of the *Gipr* in bone marrow (BM) lineages and examined functional roles for the GIPR in control of hematopoiesis. Bone marrow responses were studied in (i) mice fed regular or energy-rich diets, (ii) mice treated with hematopoietic stressors including acute 5-fluorouracil (5-FU), pamsaccharide (LPS), and Pam3CysSerLys4 (Pam3CSK4), with or without pharmacological administration of a GIPR agonist, and (iii) mice with global ($Gipr^{-/-}$) or selective deletion of the GIPR ($Gipr^{Tie2-/-}$) with and without bone marrow transplantation (BMT).

Results: *Gipr* is expressed within T cells, myeloid cells, and myeloid precursors; however, these cell populations were not different in peripheral blood, spleen, or BM of $Gipr^{-/-}$ and $Gipr^{Tie2-/-}$ mice. Nevertheless, gain and loss of function studies revealed that GIPR signaling controls the expression of BM Toll-like receptor (TLR) and Notch-related genes regulating hematopoiesis. Loss of the BM GIPR attenuates the extent of adipose tissue inflammation and dysregulates the hematopoietic response to BMT. GIPR agonism modified BM gene expression profiles following 5-FU and Pam3CSK4 whereas loss of the *Gipr* altered the hematopoietic responses to energy excess, two TLR ligands, and 5-FU. However, the magnitude of the cellular changes in hematopoiesis in response to gain or loss of GIPR signaling was relatively modest.

Conclusion: These studies identify a functional gut hormone-BM axis positioned for the transduction of signals linking nutrient availability to the control of TLR and Notch genes regulating hematopoiesis. Nevertheless, stimulation or loss of GIPR signaling has minimal impact on basal hematopoiesis or the physiological response to hematopoietic stress.

Keywords Glucose-dependent insulinotropic polypeptide receptor; Bone marrow; Hematopoiesis; Myeloid cells; Inflammation

1. INTRODUCTION

Enteroendocrine cells (EECs) sense nutrients and play important roles as first responders to enable nutrient assimilation and maintenance of energy balance. Among the most extensively characterized EEC hormones are glucose-dependent insulinotropic polypeptide (GIP) and glucagon-like peptide 1 (GLP-1), secreted by gut K and L cells, respectively. Both GIP and GLP-1 communicate with islet cells to control hormone secretion and glucose metabolism within minutes of meal ingestion [1]. Notably, GLP-1 acts beyond the pancreas to reduce food intake, inhibit gastrointestinal motility, and attenuate inflammation, actions consistent with limiting excess energy intake [2]. The actions of GLP-1 extend to cardioprotection [3,4], supporting the clinical use of GLP-1R (GLP-1 Receptor) agonists for the treatment of type 2 diabetes (T2D) and, more recently, obesity [2].

The extrapancreatic actions of GIP encompass the central nervous system, the skeleton, the cardiovascular system, and adipose tissue [1]. GIP Receptor (GIPR) coagonists such as tirzepatide [5] are being studied in phase 3 clinical trials for the treatment of T2D, and GIPR antagonists are being explored for the treatment of metabolic disorders, including obesity [6,7]. Accordingly, delineating the consequences of enhanced or diminished GIPR signaling in peripheral tissues has immediate translational relevance. Within the brain, both gain and loss of GIPR signaling reduce food intake, actions mediated in part via the control of leptin sensitivity [8,9]. GIP also exerts anabolic actions within white adipose tissue (WAT) [10,11], and the whole body inactivation of the *Gipr* or GIPR antagonism promotes resistance to diet-induced obesity associated with reductions in adipose tissue mass [12–14].

GIPR is also expressed within multiple bone cell lineages [15,16] and in bone marrow-derived cells, predominantly within a subset of monocytes and macrophages [17–19]. Notably, $Gipr^{-/-}$ mice exhibited defective hematopoiesis, characterized by reduced myeloid progenitors in the bone marrow (BM) and decreased numbers of

Lunenfeld-Tanenbaum Research Institute, Mt. Sinai Hospital, University of Toronto, ON, M5G 1X5, Canada

[1] Current address: Ottawa Heart Institute, University of Ottawa, 40 Ruskin Street, Room H3228, Ottawa, ON, Canada K1Y 4W7.

*Corresponding author. Mt. Sinai Hospital, 600 University Ave Mailbox 39, TCP5-1004, Toronto, ON, M5G 1X5. Canada. E-mail: drucker@lunenfeld.ca (D.J. Drucker).

Received April 21, 2020 • Revision received April 27, 2020 • Accepted April 28, 2020 • Available online 7 May 2020

https://doi.org/10.1016/j.molmet.2020.101008

circulating monocytes and macrophages [20]. As both GIPR coagonists and antagonists are being explored clinically for the treatment of metabolic disorders [7], the impact of GIPR signaling on hematopoiesis in normal and pathophysiological contexts has translational relevance. Here, we assessed the importance of the murine GIPR for hematopoiesis and the control of BM and adipose tissue inflammation under basal conditions and after exposure to an energy-rich diet. Due to the importance of Toll-like receptor (TLR) and Notch signaling for the control of hematopoiesis [21–26], we also assessed whether GIPR signaling regulates these pathways, using both gain and loss of function strategies. Furthermore, we studied whether the manipulation of GIPR signaling modifies the response to hematopoietic stressors including acute 5-Fluorouracil (5-FU), Lipopolysaccharide (LPS), Pam3CysSerLys4 (Pam3CSK4), and the success of bone marrow transplantation (BMT). Our results show that the *Gipr* is essential for the expression of BM genes regulating hematopoiesis and adipose tissue inflammation, and the loss of the BM GIPR alters the hematopoietic response to BMT. Nevertheless, gain or loss of GIPR signaling does not have a major impact on the bone marrow response to hematopoietic stress in mice.

2. MATERIALS AND METHODS

2.1. Animals

Mice were maintained on a 12 h light/dark cycle at room temperature, with free access to food and water, except when indicated. Mice were fed either a standard rodent chow diet (RCD) (18% kcal from fat, 2018 Harlan Teklad, Mississauga, ON, Canada) or a high-fat diet (HFD) (45% kcal from fat, D12451i, Research Diets, New Brunswick, NJ, USA). The generation and characterization of $Gipr^{-/-}$ as well as $Gipr^{Flox/Flox}$ mice were previously described [10,27]. B6.Cg-Tg(Tek-cre)1Ywa/J (*Tie2-cre*) mice were obtained from Jackson Laboratories. As described for the B6.Cg-Tg(Tek-cre)1Ywa/J strain [28], germline deletion was prevented by restricting Cre expression to male breeders. To generate $Gipr^{Tie2-/-}$ mice, *Tie2-cre* hemizygous mice were bred with floxed *Gipr* mice ($Gipr^{Flox/Flox}$). WT B6.SJL-Ptprca $Pepc^{b}$/BoyJ CD45.1+ mice for bone marrow transplant experiments were obtained from Jackson Laboratories. Animals were treated with 24 nmol/kg [DAla2]-GIP (Chi Scientific, Maynard, MA, USA) twice a day (9 am and 5 pm) for a total of 8 days when combined with 5-FU and a total of 6 days when combined with LPS and Pam3CSK4. Alternatively, 150 mg/kg of 5-FU (provided by Mount Sinai Hospital Pharmacy) was given once weekly (for a total of 2–3 doses as indicated). LPS 35 μg (Sigma–Aldrich, Cat# L3024, Oakville, ON, Canada) was administered for a total of three doses, administered 48 h apart. Pam3CSK4 (InvivoGen, Cat# tlr-pms, San Diego, CA, USA) 100 μg per injection was administered for a total of three doses, administered 48 h apart. Phosphate-buffered saline was administered as a vehicle control. Experiments were carried out in groups of male or female mice on a C57BL/6J background. As no differences were found between the control groups (*Wild type*, $Gipr^{Flox/Flox}$, and *Tie2-cre*), only data from *Tie2-cre* mice are shown as a control (unless otherwise stated).

2.2. Body composition using magnetic resonance imaging (MRI)

Body composition (fat and lean mass) was measured prior to and every 4 weeks after placing mice on an HFD, using an Echo MRI nuclear magnetic resonance system (Echo Medical Systems, Houston, TX, USA).

2.3. Blood and tissue collection

For terminal studies, mice were sacrificed by CO_2 inhalation, blood was obtained by cardiac puncture, and tissues were dissected and immediately frozen in liquid nitrogen. All blood samples (50–100 μL) for measuring insulin, GLP-1, GIP, and triglycerides at indicated time points during metabolic tests were collected from tail vein into lithium-coated Microvette tubes (Sarstedt, Numbrecht, Germany) and mixed with a 10% volume of TED (5000 kIU/mL Trasylol (Bayer), 32 mM EDTA, and 0.01 mM Diprotin A (Sigma)). Samples were kept on ice and plasma was collected by centrifugation and stored at −80 °C. When blood was collected to perform a complete blood count analysis, ~200 μL was collected from the tail vein into EDTA-coated Microvette tubes (Sarstedt, Numbrecht, Germany) and kept at room temperature (RT) prior to analysis.

2.4. Glucose, insulin, and lipid tolerance tests

All metabolic tests were performed after a 4–5 h fast (~9 am–1 pm). For oral and intraperitoneal glucose tolerance tests (OGTT and IPGTT, respectively), D-Glucose (2 g/kg; Sigma, Oakville, ON, Canada) was administered by oral gavage (OGTT) or IP injection (IPGTT). During insulin tolerance tests (ITTs), animals received a single IP injection of 0.75 U/kg BW of insulin (Humalog, VL7510, Eli Lily, Scarborough, ON, Canada). Blood glucose was measured in tail vein samples using a handheld glucose meter (Contour, Bayer, Mississauga, ON, Canada) at baseline (time 0) and 15, 30, 45, 60, 90, and 120 min after glucose or insulin administration. For oral lipid tolerance tests (OLTTs), animals received a 200 μL oral gavage of olive oil (Sigma) at time 0, and blood samples were collected from the tail vein prior to and 1, 2, and 3 h after olive oil gavage.

2.5. Hormone and enzymatic assays

Plasma insulin (Ultrasensitive Mouse Insulin ELISA, Cat# 80-INSMSU-E01 Alpco Diagnostics, Salem, NH, USA), total GLP-1 (Meso Scale Diagnostics, Cat# K150JVC-2 Rockville, MD, USA), and total GIP (Crystal Chem, Cat# 81517, Elk Grove Village, IL, USA) levels were assessed in plasma samples collected at baseline (time 0), 5, 15, or 30 min after glucose or insulin administration during metabolic tests, as indicated. Triglycerides (TGs) were assayed using the Trig-GB kit (Cat# 11877771216, Roche, Mississauga, ON, Canada), at baseline (time 0), 1, 2, and 3 h after oral lipid administration

2.6. Cell preparation for flow cytometry analysis and sorting

Samples for cell isolation from peripheral blood, spleen, or bone marrow were obtained from 8-week-old females. Immediately following sacrifice by CO_2 inhalation, ~700–800 μL of blood was obtained by cardiac puncture and added to 13 mL of red blood cell lysis solution (RBC solution) (BioLegend, Cat# 420301, San Diego, CA, USA) for 14 min at RT with shaking, and cells were pelleted by centrifugation at 1800 rpm, for 5 min at 4 °C. To isolate spleen cells, the entire spleen was placed in a 70 μM cell strainer (Falcon, Cat# 352350, NY, USA) and gently ground through the strainer using the plunger of a 1 mL syringe (BD Biosciences, Cat# 309659, NJ, USA). Spleen cells were rinsed through the cell strainer with three rounds of 3 mL of Iscove's Modified Dulbecco's Medium (IMDM) (STEMCELL Technologies, Cat# 36150, Vancouver, BC, Canada). To isolate bone marrow cells, two femurs were crushed in 3 mL of IMDM medium using a mortar and pestle and filtered through a 70 μM cell strainer. This process was repeated two more times. Spleen or bone cells were pelleted and resuspended in 1–5 mL of FACS buffer (PBS containing 2 mM EDTA, 25 mM HEPES, and 2% FCS) and then lysed with RBC solution for 5 min at RT. The lysis was stopped with 5 mL of FACS

buffer and cells were pelleted by centrifugation (1800 rpm 5 min at 4 °C). Cells from spleen and bone marrow were resuspended with FACS buffer and filtered using a 5 mL polystyrene round-bottom tube with a cell strainer cap (Falcon, Cat# 352235, NY, USA) to obtain a single-cell solution. Fc receptors were blocked using TruStain fcX™ (CD16/32 antibody) (BioLegend) for 10 min. Cells were then incubated for 30 min with two panels of fluorophore-conjugated antibodies (Tables S1 and S2), to identify immune cell populations, specifically (i) a lymphocyte-myeloid panel (APC-CD45, FITC-CD45R/B220, FITC-Ly6G/Ly6C (Gr-1), FITC-CD18, PE-CD45R/B220, PE-CD8a, and PE-CD4) and (ii) a monocyte-neutrophil panel. To isolate hematopoietic stem and progenitor cells (HSPCs) from bone marrow, 2–4 x 10^7 cells were resuspended in 1 mL of PBS containing 2 mM EDTA and 0.5% BSA and were incubated for 10 min at 4 °C according to the manufacturer's instructions for the mouse direct lineage cell depletion kit (Miltenyi Biotec, Cat# 130-110-470, Auburn, CA, USA). Lineage-negative cells were separated using LS columns (Miltenyi Biotec, Cat# 130-042-401, Auburn, CA, USA) and a QuadroMACS™ separation unit (Miltenyi Biotec, Cat# 130-090-976, Auburn, CA, USA). Cells were then incubated for 30 min with the HSPC panel of fluorophore-conjugated antibodies (Biotin-Lineage cocktail (ter119, CD11b, Gr-1, CD3e, and B220), Alexa Fluor 488-Sca-1, APC/Fire750-cKit (CD117), PE-CD34, BV510-CD16/32, BV421-CD135, PE/Cy7-CD150 (SLAM), and APC-CD48), followed by a 30 min incubation with Streptavidin-PE-Cy5. Target populations of live cells (DAPI+) were isolated using a MoFlo Astrios EQ Cell Sorter equipped with 355 nm, 405 nm, 488 nm, 560 nm, and 642 nm lasers (Beckman Coulter, Miami, FL, USA) or analyzed using a Gallios flow cytometer equipped with 405 nm, 488 nm, 561 nm, and 638 nm lasers (Beckman Coulter). B cells are defined as $CD45^+$, $CD45R/B220^+$, Gr-1 $(Ly\text{-}6G/Ly\text{-}6C)^-$, $CD18^-$, $CD8a^-$, and $CD4^-$. T cells are $CD45^+$, $CD45R/B220^-$, Gr-1 $(Ly\text{-}6G/Ly\text{-}6C)^-$, $CD18^-$, $CD8a^+$, and $CD4^+$; myeloid (M) cells are gated as $CD45^+$, $CD45R/B220^-$, Gr-1 $(Ly\text{-}6G/Ly\text{-}6C)^+$, $CD18^+$, $CD8a^-$, and $CD4^-$. In bone marrow samples, LK is Lin^- $cKit^+$ and LKS is Lin^- $cKit^+$ $Sca\text{-}1^+$. Short-term and long-term hematopoietic stem cells (ST-HSC and LT-HSC, respectively) are Lin^- $cKit^+$ $Sca\text{-}1^+$ $CD135^-$, $CD48^-$, and $CD150^{DIM}$ (ST) and $CD150^{HI}$ (LT), while multipotent progenitor (MPP) cells are Lin^- $cKit^+$ $Sca\text{-}1^+$ $CD135^-$ and $CD48^+$. Common lymphoid progenitor (CLP) cells are defined as Lin^- $cKit^+$ $Sca\text{-}1^+$ $CD135^+$ $CD150^-$. Common myeloid progenitor (CMP) cells are Lin^- $cKit^+$ $Sca\text{-}1^-$ $CD34^+$ $CD16/32^-$, granulocyte-monocyte progenitor (GMP) cells are Lin^- $cKit^+$ $Sca\text{-}1^-$ $CD34^+$ $CD16/32^+$, and megakaryocyte-erythroid progenitor (MEP) cells are Lin^- $cKit^+$ $Sca\text{-}1^-$ $CD34^-$ $CD16/32^-$ (see Tables S1 and S2 for details).

2.7. Colony-forming unit (CFU) assay

MethoCult CFU assays were performed with MethoCult™ GF M3434 (STEMCELL Technologies, Cat# 03434, Vancouver, BC, Canada) according to the manufacturer's protocol. Briefly, MethoCult was thawed at 4 °C overnight and mixed. To isolate bone marrow cells, two femurs from 8-week-old female mice were crushed and washed three times with 3 mL of IMDM medium containing 10% Fungizone®-Amphotericin B (250 μg/mL) (Gibco, Cat# 15290–018) and filtered through a 70 μM cell strainer, all under sterile conditions. Cells were lysed with RBC solution for 5 min at RT and resuspended in 3 mL of IMDM medium to a concentration of 2 × 10^5 cells/mL. A one-tenth volume of the prepared cells was mixed with 3 mL of MethoCult by vortexing. Cells were plated in duplicate in 35 mm grid dishes (Sarstedt, Cat# 83.3900.002, Newton, NC, USA) using a 3 cc syringe (STEMCELL Technologies, Cat# 28240, Vancouver, BC, Canada) and a 16-gauge blunt-end needle (STEMCELL Technologies, Cat# 28110, Vancouver, BC, Canada). Cells were incubated in a humidified chamber at 37 °C and 5% CO_2 for 7 (for replating purposes) or 10 days, and then colonies were identified and counted under a bright field microscope. For replating assays, after 7 days of the initial plating, marrow cells were collected by pipetting and washed with 9 mL of IMDM medium. Cells were counted and plated in equal proportions as described above. Total colony numbers were compared between WT and $Gipr^{-/-}$ or *Tie2-cre* and $Gipr^{Tie2-/-}$ mice.

2.8. Bone marrow transplantation

Bone marrow chimeras were generated by irradiating 8-week-old WT B6.SJL-Ptprca $Pepc^b$/BoyJ CD45.1+ recipient males, obtained from Jackson Labs (1,100 cGy, split into two equal doses separated 4 h apart) followed by tail vein injection of 5 × 10^6 congenic bone marrow cells from WT C57BL6/J or $Gipr^{-/-}$ donor males, as described [29,30]. The efficiency of reconstitution was assessed by flow cytometry analysis (Gallios, Beckman Coulter) of tail vein blood every 4 weeks until sacrifice at 16 weeks after BMT. For flow cytometry, CD45.1-PE-Cy7, CD45.2-APC, and CD45.2-FITC antibodies were added to the lymphocyte-myeloid and monocyte-neutrophil panels described above (see Tables S1 and S2 for details).

2.9. RNA isolation and gene expression analysis

Tissue samples and cell pellets were homogenized in Tri Reagent (Molecular Research Center, Cincinnati, OH, USA) using a TissueLyser II system (Qiagen, Germantown, MD, USA), for the extraction of total RNA. First-strand cDNA was synthesized from DNase I-treated total RNA using the SuperScript III and random hexamers (Thermo Fisher Scientific, Markham, ON, Canada). Reverse transcription reactions were carried out for 10 min at 25 °C, 50 min at 50 °C, and an additional 15 min at 70 °C. Gene expression levels were quantified by real-time quantitative PCR (RT-qPCR) using a QuantStudio System and TaqMan Gene Expression Master Mix and Assays (Thermo Fisher Scientific). Oligonucleotides were purchased from Thermo Fisher Scientific. Primer sequences are provided in Table S3. qRT-PCR data were analyzed by the $2^{-\Delta\Delta Ct}$ method, and expression levels for each gene were normalized to *Ppia* (peptidylprolyl isomerase A-cyclophilin A).

2.10. Quantification and statistical analysis

Data are represented as the mean ± SD or as the mean ± SEM, as indicated. Statistical comparisons were made by one- or two-way ordinary ANOVA followed by Bonferroni post hoc or by unpaired two-tailed Student's *t*-test (only when two conditions) using GraphPad Prism version 8 software (San Diego, CA, USA). The Log-rank (Mantel–Cox) test was used to evaluate survival rates. A P value ≤ 0.05 was considered statistically significant.

3. RESULTS

3.1. Toll-like receptor and notch genes are dysregulated in BM from HFD-fed $Gipr^{-/-}$ mice

TLRs are expressed in a variety of cell populations, including immune cells and nonimmune cells, such as HSPCs and endothelial cells [21–23]. When engaged, they regulate the proliferation, mobilization, and differentiation of HSC (Hematopoietic Stem Cells) and committed progenitors [21,24–26]. Recent studies reported a reduction in bone marrow progenitors and circulating myeloid cells in $Gipr^{-/-}$ mice [20]. To determine whether this defect may reflect alterations in TLR signaling, we studied the expression of TLRs and downstream effectors,

MyD88 and *Ticam1*, in BM cells from 8- to 13-week-old RCD-fed *Gipr*$^{-/-}$ mice. Only the levels of *Tlr8* and *Tlr13* mRNA were downregulated in RNA from *Gipr*$^{-/-}$ mice (Figure 1A). In contrast, the BM from HFD-fed *Gipr*$^{-/-}$ mice exhibited reduced levels of *Tlr4*, *Tlr5*, *Tlr6*, *Tlr7*, *Tlr9*, *Tlr13, MyD88*, and *Ticam1* (Figure 1B).

We next analyzed the BM expression of Notch receptors (*Notch1*, *Notch2*, *Notch3*, and *Notch4*), ligands (*Jag1* and *Dkk*), and targets (*Hes1* and *Hes3*), genes important for hematopoiesis [31]. Only the levels of *Notch2* were reduced in the BM from RCD-fed mice (Figure 1C). However, the levels of *Notch1*, *Notch2*, *Notch3*, *Jag1*, and *Hes1* mRNA transcripts were lower in BM from HFD-fed *Gipr*$^{-/-}$ mice (Figure 1D). Hence, HFD-fed, but not RCD-fed *Gipr*$^{-/-}$ mice, display an impaired expression of multiple BM genes within the TLR and Notch pathways.

3.2. *Gipr* expression is downregulated in bone marrow cells from *Gipr*$^{Tie2-/-}$ mice

To further delineate the contribution of *Gipr* to hematopoietic cell lineages, we crossed *Tie2-cre* mice with *Gipr*$^{Flox/Flox}$ to generate *Gipr*$^{Tie2-/-}$ mice (Figure S1A). Tunica intima endothelial kinase 2 (Tie2/Tek) is expressed in endothelial cells, within all progenitor and several differentiated hematopoietic cells, but not in the bone marrow stromal compartment [32]. *Gipr* mRNA transcripts were not reduced in the jejunum, epididymal, or mesenteric WAT of *Gipr*$^{Tie2-/-}$ mice (Figure S1B). Moreover, *Gipr* levels were very low and unchanged in lung, spleen, thymus, and lymph nodes from *Gipr*$^{Tie2-/-}$ mice, tissues with substantial contributions from hematopoietic cell lineages. Although GIPR expression has been reported in some endothelial cell lines [33], *Gipr* mRNA transcripts were not reduced in major blood vessels, specifically in the thoracic aorta and aortic arch, from *Gip*$^{Tie2-/-}$ mice (Figure S1B). In contrast, *Gipr* mRNA levels were markedly downregulated (by about 90%) in BM cells from *Gipr*$^{Tie2-/-}$ mice (Figure S1B).

Given our detection of abnormal BM expression of TLR and Notch genes in HFD-fed *Gipr*$^{-/-}$ mice (Figure 1B,D), we assessed *Gipr*$^{Tie2-/-}$ mice after 25 weeks of 45% HFD feeding. Although body weight and adiposity trended higher in *Gipr*$^{Tie2-/-}$ mice, glucose, lipid, and insulin tolerance were not different (Figures S1C—S1K), apart from a modest increase in glucose excursion after intraperitoneal glucose challenge (Figure S1I). Plasma GLP-1 levels were not different, but GIP levels were slightly higher after oral glucose in HFD-fed *Gipr*$^{Tie2-/-}$ mice, corresponding to increased insulin levels (Figures S1F—S1H).

The levels of *Gipr* mRNA were low or undetectable in circulating white blood cells (Figure 1E), relatively higher within the BM and spleen, and markedly reduced within the BM, including BM T cells and myeloid cells of *Gipr*$^{Tie2-/-}$ mice (Figure 1E). Strikingly, *Gipr* was not detectable in early bone marrow progenitor cells (LT-ST HSC, MPP), or in CLP. However, *Gipr* was expressed at low levels in the CMP lineage and in the more differentiated myeloid progenitor populations, GMP and MEP. *Gipr* expression in these cell populations was markedly reduced in *Gipr*$^{Tie2-/-}$ mice (Figure 1E). Tissue weights from spleen, iWAT, eWAT, mWAT, and BAT were not different between *Tie2-cre* and *Gipr*$^{Tie2-/-}$ mice (Figure S1L).

3.3. TLR and notch gene expression and hematopoiesis are not dysregulated in *Gipr*$^{Tie2-/-}$ mice

Body weight, spleen and femur weights, femur length, and spleen and femur cellularity were not different in *Gipr*$^{-/-}$ and *Gipr*$^{Tie2-/-}$ mice (Figures S2A—S2F). Flow cytometry analysis (Figures S3A—S3D and Tables S1-S2) revealed similar frequencies of CD45+ cells, and no differences were observed in populations of T cells, B cells, or myeloid cells in peripheral blood, spleen, or BM from *Gipr*$^{-/-}$ and *Gipr*$^{Tie2-/-}$ mice (Figures S2G—S2I). BM RNA from RCD-fed and HFD-fed *Gipr*$^{Tie2-/-}$ mice did not reveal differences in the expression of TLR or Notch pathway genes (Figure 1F—I).

We next analyzed HSPCs using a panel of lineage markers (TER-119, CD11b, Ly-6G/Ly-6C (Gr-1), CD3e, and CD45R/B220) to discriminate between differentiated and nondifferentiated cells in the BM (Figure S3D and Tables S1-S2). Lineage-negative (Lin-) cells were not different in *Gipr*$^{-/-}$ or *Gipr*$^{Tie2-/-}$ animals (Figure S2J), and no differences were observed in Lin-cKit + Sca1+ (LKS) or in Lin-cKit + Sca1- (LK) stem cell populations (Figure S2K). Similarly, the LT-ST HSC population and the multipotent progenitor (MPP) cell frequencies were comparable (Figure S2L), and no differences were found in CLP, CMP cells, or the differentiated myeloid progenitor (GMP and MEP) cell populations (Figures S2M-S2N).

To discern the importance of GIPR signaling for hematopoiesis, we performed colony-forming unit (CFU) assays, a widely used technique to assess the ability of HSPC cells to proliferate and differentiate *in vitro,* using BM cells from femurs of 8-week-old female *Gipr*$^{-/-}$ and *Gipr*$^{Tie2-/-}$ mice. No major differences were observed in cell populations within colonies established from both *Gipr*$^{-/-}$ and *Gipr*$^{Tie2-/-}$ mice (Figures S2O—S2S). However, at 10 days, the granulocyte-macrophage (GM) population was increased in colonies originating from *Gipr*$^{-/-}$ compared to WT mice, without differences in the proportion of the other assessed populations (Figure S2P). In contrast, no changes were observed in colonies propagated from *Gipr*$^{Tie2-/-}$ mice (Figure S2P). A decrease in the granulocyte (G) population was observed in both *Gipr*$^{-/-}$ and *Gipr*$^{Tie2-/-}$ mice at 14 days (Figure S2Q). However, this decrease had no impact on other cell populations, nor were abnormalities observed at subsequent replating time points. Taken together, these results indicate that, despite the reduction of *Gipr* expression in different BM cell populations, loss of GIPR signaling within the Tie2+ lineage did not impact hematopoiesis.

3.4. Reconstitution of hematopoiesis after bone marrow transplant does not require the GIPR

To further probe the importance of the GIPR for hematopoiesis, we performed a noncompetitive BMT to assess HSPC repopulation capacity. BM cells from WT or *Gipr*$^{-/-}$ female donors (CD45.2) were transplanted into irradiated WT male recipients (CD45.1). Mice were maintained on RCD or HFD, and the frequency of cell populations and gene expression were examined 16 weeks after BMT (Figure S4A). *Gipr* expression was reduced in BM and spleen cells, but not in fat depots of RCD-fed *Gipr*$^{-/-}$ BM recipients, consistent with successful BMT (Figure S4B). Body weights were not different between genotypes in transplanted mice (Figure S4C). Repopulation capacity in peripheral blood (Figure S4D) was also similar between groups. Tissue weights were not different in *Gipr*$^{-/-}$ BM recipients, and no differences in femur length or femur and spleen cellularity were observed (Figure S4E).

To determine if prolonged high-fat feeding, a condition associated with dysregulation of TLR and Notch gene expression in *Gipr*$^{-/-}$ mice (Figure 1A—D), as well as increased circulating levels of GIP [1], could modify hematopoiesis after BMT, mice were placed on a 45% HFD for 14 weeks, starting two weeks following BMT (Figure S4A). *Gipr* expression was reduced in BM and spleen cells of HFD-fed *Gipr*$^{-/-}$ BM recipients, but not in adipose tissues (Figure S4F). Body weight gain was not different between groups (Figure S4G). The repopulating capacity of BM assessed through the analysis of peripheral blood was not different (Figure S4H), and tissue weights were similar in BM recipients

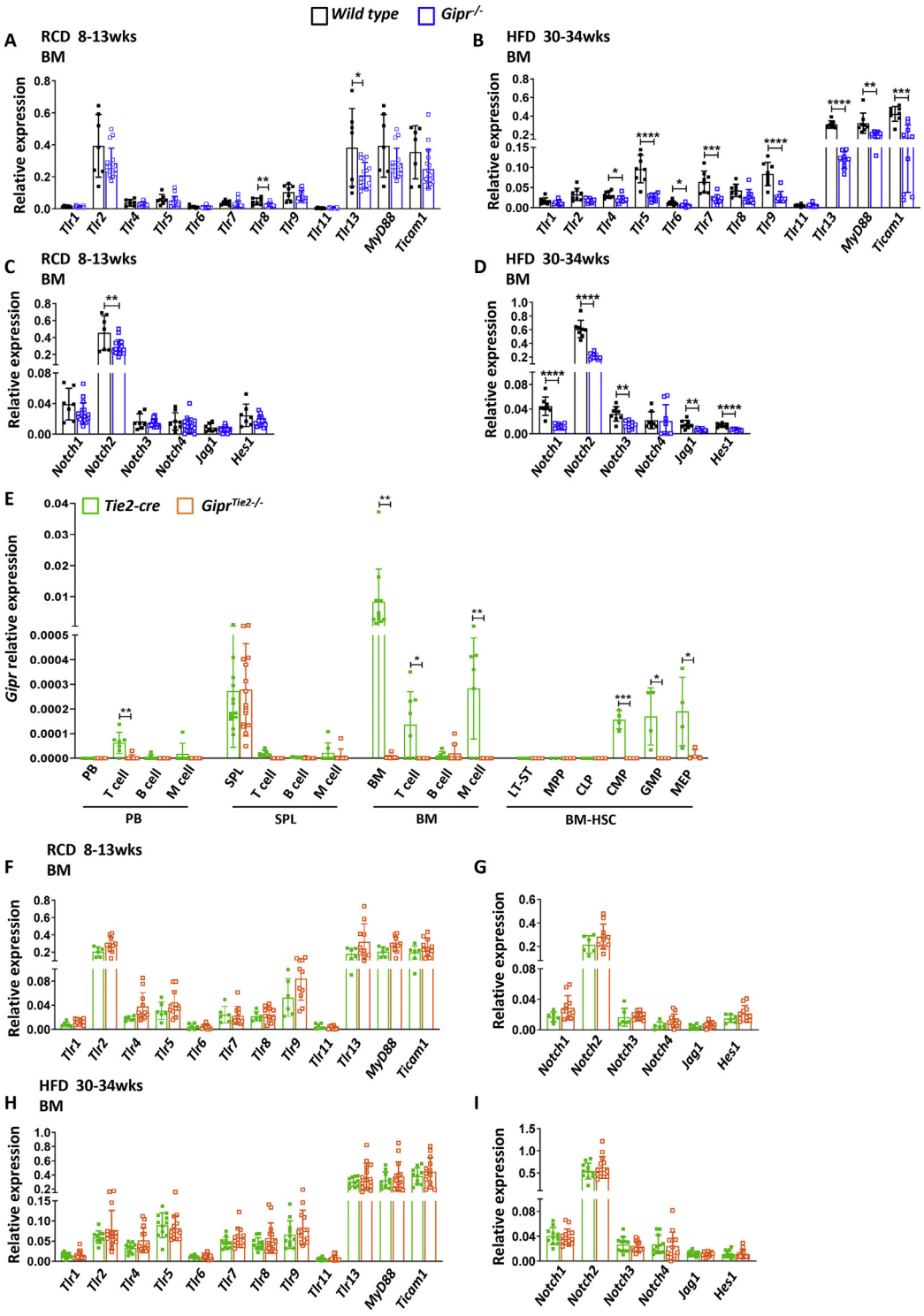

Figure 1: TLR and Notch expression is downregulated in bone marrow cells of HFD-fed *Gipr*$^{-/-}$ mice. mRNA levels of the indicated TLR and Notch signaling-related genes, relative to *Ppia* gene expression, were assessed in isolated BM cells from 8- to 13-week-old RCD-fed (n = 6–17/group) (A, C) and from 30- to 34-week-old HFD-fed (n = 8–14/group) (B, D) WT and *Gipr*$^{-/-}$ male mice. (E) *Gipr* mRNA levels, relative to *Ppia*, in the indicated cell populations isolated by flow cytometry from peripheral blood, spleen, and bone marrow of 8-week-old *Tie2-cre* and *Gipr*$^{Tie2-/-}$ female mice. mRNA levels of the indicated TLR and Notch signaling-related genes, relative to *Ppia* gene expression, were assessed in isolated BM cells from 8- to 13-week-old RCD-fed (n = 6–17/group) (F,G) and from 30- to 34-week-old HFD-fed (n = 8–14/group) (H, I) *Tie2-cre* and *Gipr*$^{Tie2-/-}$ male mice. Data are presented as the mean ± SD. $^{*}P \leq 0.05$, $^{**}P \leq 0.01$, $^{***}P \leq 0.001$, and $^{****}P \leq 0.0001$. RCD: regular chow diet; HFD: high-fat diet; wks: weeks; BM: bone marrow; PB: peripheral blood; SPL: spleen; M cells: myeloid cells; HSC: hematopoietic stem cells; ST-HSC: short-term hematopoietic stem cells; LT-HSC: long-term hematopoietic stem cells; MPP: multipotent progenitor; CLP: common lymphoid progenitor; CMP: common myeloid progenitor; GMP: granulocyte-monocyte progenitor; MEP: megakaryocyte-erythroid progenitors.

(Figure S4I). Interestingly, spleen cellularity, but not weight, was decreased in *Gipr*$^{-/-}$ BM-transplanted mice (Figure 2A).

The analysis of BM mRNA transcripts corresponding to genes important for TLR and Notch signaling revealed only a few differences in *Gipr*$^{-/-}$ BM-transplanted mice (Figure 2B—E). The levels of *Tlr11* and *Hes1* were reduced in RCD-fed mice (Figure 2B and C), while *Tlr1* and *Tlr5* mRNA transcripts were decreased in *Gipr*$^{-/-}$ BM recipient mice fed an HFD (Figure 2D and E). The distributions of lymphocytes versus myeloid cell populations were not different in peripheral blood of RCD-fed mice; however, the proportion of CD11b + cells was increased (Figure 2F). Ly6C- cells were increased and circulating proinflammatory monocytes (Ly6C^{++}) were decreased in *Gipr*$^{-/-}$ BM recipients (Figure 2F).

No differences in proportions of CD45+ cells or population frequency distribution of lymphocytes and myeloid cells in spleen or BM were observed (Figure 2G and H). However, monocytes (Ly6C^{+}) were decreased in both spleen and BM cells of *Gipr*$^{-/-}$ BM recipients, Ly6C- cells were increased in the spleen, while the numbers of CD11b+ and proinflammatory monocytes (Ly6C^{++}) were increased in BM (Figure 2G and H). No differences were found in the lineage-negative HSC population (Figure S5A), LKS and LK cell frequencies, LT-ST HSC or MPP progenitors (Figures S5B-S5C), or the CLPs (Figure S5D). The GMP cell population was increased in *Gipr*$^{-/-}$ BM recipients, but CMP and MEP populations were not perturbed (Figure 2I).

The distribution of lymphocytes versus myeloid cell populations was similar in peripheral blood of HFD-fed WT and *Gipr*$^{-/-}$ BM recipients (Figure 2J). Nevertheless, the levels of circulating neutrophils (CD115^{-}) and inflammatory monocytes (LyC6^{++}) were reduced and the numbers of anti-inflammatory monocytes (LyC6-) were increased in *Gipr*$^{-/-}$ BM recipients (Figure 2J). The analysis of the spleen revealed small differences in lymphoid and myeloid cell populations, including a slight increase in B cells and M cells, and reduced numbers of T cells in *Gipr*$^{-/-}$ BM recipients fed in an HFD (Figure 2K). Ly6C- cell populations were increased, while inflammatory monocytes (Ly6C+) were reduced (Figure 2K). BM cell populations were not different (Figure S5E). The BM lineage-negative population and LKS frequencies were comparable, and LK cell numbers were unchanged (Figures S5F-S5G). The numbers of MPP progenitors were lower; however, the proportions of LT-ST HSC cells were similar in *Gipr*$^{-/-}$ BM recipient mice (Figure 2L). Common lymphoid and myloid progenitors (CLP, CMP) populations were similar (Figure S5H,I).

3.5. GIPR agonism modifies TLR and notch pathway responses to 5-FU and Pam3CSK4

We next asked whether the GIPR was important for adaptive hematopoiesis in response to (i) the chemotherapeutic agent 5-FU and (ii) two distinct TLR ligands, LPS acting through TLR4 and Pam3CSK4 acting via TLR1/2. 5-FU is a chemotherapeutic agent that activates HSPCs while eliminating proliferative myeloid cells [34], whereas LPS and Pam3CSK4 engage TLR receptors to regulate HSPC proliferation and myelopoiesis [25,35]. Interestingly, plasma GIP levels were increased after 5-FU and trended higher after LPS administration in WT mice (Figure S6A). Baseline GIP levels were higher in *Gipr*$^{-/-}$ mice and did not increase further after 5-FU or LPS (Figure S6A), whereas GIP levels were not different after the Pam3CSK4 administration (Figure S6A).

Subsequently, we examined whether genes important for TLR signaling were dysregulated in isolated BM cells from WT and *Gipr*$^{-/-}$ mice following the administration of 5-FU, LPS, or Pam3CSK4 (Figure S6B). The majority of mRNA transcripts examined did not exhibit genotype-dependent regulation after 5-FU, LPS, or Pam3CSK4, with the exception of *MyD88*, which was markedly upregulated by Pam3CSK4 only in BM from *Gipr*-deficient mice, and *Tlr6,* which was upregulated in BM from WT but not *Gipr*$^{-/-}$ BM, whereas *Tlr1* was induced in *Gipr*$^{-/-}$ mice BM after 5-FU (Figure S6B).

To assess whether the activation of GIPR signaling modified the BM gene expression profile response to 5-FU, LPS, or Pam3CSK4, we coadministered the degradation-resistant GIPR agonist, [DAla2]-GIP [10,36]. Interestingly, BM expression of *Tlr2*, *Tlr4*, *Tlr5*, *Tlr8*, *Tlr9*, *Tlr13, Notch1, Jag1* and *Notch2* and the downstream target, *Ticam1*, were differentially regulated by the coadministration of [DAla2]-GIP in 5-FU-treated mice (Figure 3A). Specifically, 5-FU and [DAla2]-GIP cotreatment increased the levels of *Tlr4*, *Tlr5*, *Tlr8*, and *Notch1* expression relative to basal levels seen with [DAla2]-GIP alone. Coadministration of LPS and [DAla2]-GIP had relatively little effect on BM gene expression profiles, relative to LPS alone (Figure S6C). Conversely, cotreatment with [DAla2]-GIP attenuated changes in BM levels of *Tlr1*, *Tlr8*, *Tlr13*, *MyD88*, and *Ticam1* mRNA transcripts observed with Pam3CSK4 alone (Figure 3B). Interestingly, *Tlr9* expression was not affected by Pam3CSK4 alone, yet mRNA levels decreased with concomitant [DAla2]-GIP administration (Figure 3B).

3.6. *Gipr* is dispensable for adaptive hematopoiesis in response to 5-FU

We next examined whether the loss of *Gipr* impaired adaptive hematopoiesis. Interestingly, *Gipr*$^{-/-}$ but not *Gipr*$^{Tie2-/-}$ mice displayed better survival following 5-FU treatment (Figure S7A), consistent with the findings of improved survival of stressed *Gipr*$^{-/-}$ mice in response to myocardial ischemia [37]. Hence, WT and *Gipr*$^{-/-}$ mice were examined in more detail after 5-FU administration (Figure S7B). No differences in spleen or femur weight or cellularity were detected in 5-FU-treated WT versus *Gipr*$^{-/-}$ mice; however, body weight trended lower in 5-FU-treated *Gipr*$^{-/-}$ mice (Figures S7C—S7G). Peripheral blood myeloid cell populations were reduced after 5-FU, whereas T cells were increased (Figure S7H). Splenic B and T cell numbers, as well as myeloid cell numbers, were not different in 5-FU-treated mice (Figure S7I). B and T cell numbers were also increased after 5-FU in WT and *Gipr*$^{-/-}$ BM (Figure S7J), whereas BM myeloid cell numbers trended lower or were reduced in 5-FU-treated WT and *Gipr*$^{-/-}$ mice, respectively (Figure S7J).

No differences were observed in the proportions of BM Lin- cells (Figure S7K); however, LK and LKS cell numbers were reduced in the BM of 5-FU-treated mice, independent of the genotype (Figure S7L). LT-ST HSC cells were decreased while MPP cells were increased after 5-FU; however, no differences were observed in *Gipr*$^{-/-}$ versus WT mice (Figure S7M). The CLP population decreased similarly in both 5-FU treated groups (Figure S7N), whereas the levels of CMP, GMP, and MEP cells were not significantly different (Figure S7O).

We next treated mice with [DAla2]-GIP and examined the hematopoietic response to 5-FU (Figure S8A). Body weight was reduced after 5-FU, but no differences in spleen or femur weights or femur cellularity were observed in mice treated with [DAla2]-GIP (Figure S8B-F). Administration of [DAla2]-GIP for 8 days did not alter the populations of B cells, T cells, or myeloid cells in peripheral blood (Figures S8G-S8H) or BM (Figure 4A) of mice treated with 5-FU. Intriguingly, the reduction in the CD115- BM population (neutrophils) was blunted in [DAla2]-GIP-treated mice (Figure 4B), whereas the majority of BM-HPSC lineages were not different (Figures S8I—S8M).

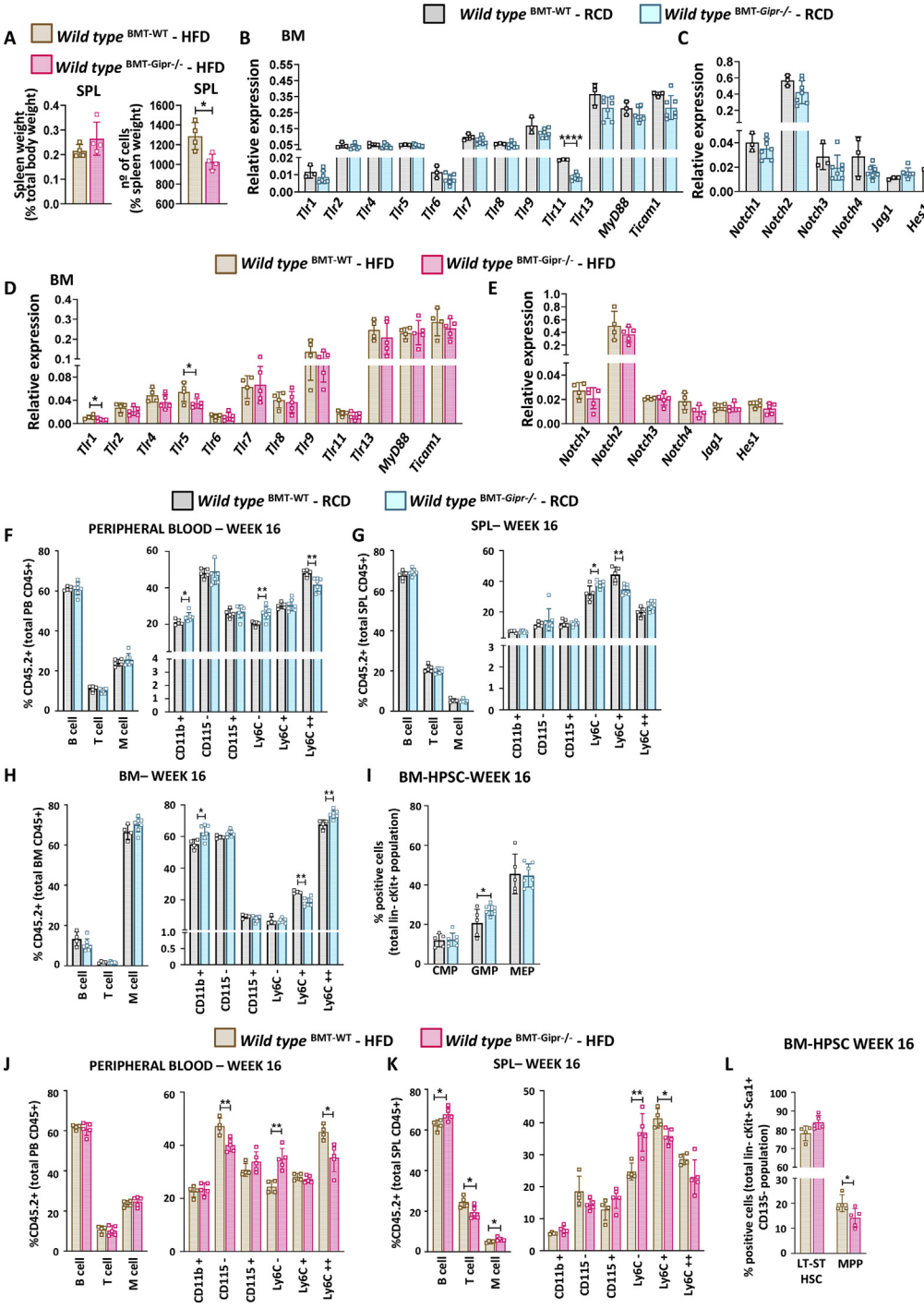

Figure 2: Hematopoietic responses after RCD or HFD feeding in mice transplanted with *Gipr*$^{-/-}$ donor BM. (A) Spleen weight, relative to body weight, and spleen cellularity from 26-week-old WT male mice that received WT (BMT-WT) or *Gipr*$^{-/-}$ (BMT-*Gipr*$^{-/-}$) bone marrow at the age of 8 weeks and were fed an HFD for 14 weeks. mRNA levels of the indicated TLR and Notch signaling-related genes, relative to *Ppia* gene expression, were assessed in isolated BM cells from 26-week-old WT male mice that received WT (BMT-WT) or *Gipr*$^{-/-}$ (BMT-*Gipr*$^{-/-}$) bone marrow at the age of 8 weeks and were fed an RCD (B, C) (n = 5–7/group) or HFD (D, E) (n = 4–5/group) for 14 weeks. Examination of B cells, T cells, and M cells and monocyte lineage cells (neutrophils and monocytes) at 16 weeks after BMT as a percentage of donor repopulated cells (CD45.2) in peripheral blood (F), spleen (G), and BM (H), and (I) frequency of CMP, GMP, and MEP cells in bone marrow at 16 weeks after BMT from male mice that received WT (BMT-WT) or *Gipr*$^{-/-}$ (BMT-*Gipr*$^{-/-}$) bone marrow at the age of 8 weeks and were fed an RCD (n = 5–7/group). Examination of B cells, T cells, and myeloid cell populations (neutrophils and monocytes) at 16 weeks after BMT as a percentage of donor repopulated cells (CD45.2) in peripheral blood (J) and spleen (K), and (L) frequency of LT-ST HSC and MPP cells in bone marrow at 16 weeks after BMT from male mice that received WT (BMT-WT) or *Gipr*$^{-/-}$ (BMT-*Gipr*$^{-/-}$) bone marrow at the age of 8 weeks and were fed an HFD for 14 weeks (n = 4–5/group). Data are presented as the mean ± SD. $^{*}P \leq 0.05$ and $^{**}P \leq 0.01$. BMT: bone marrow transplant; RCD: regular chow diet; HFD: high-fat diet; BM: bone marrow; SPL: spleen; PB: peripheral blood; M cells: myeloid cells; BM-HPSC: bone marrow hematopoietic progenitor stem cells; Lin-: lineage negative; ST-HSC: short-term hematopoietic stem cells; LT-HSC: long-term hematopoietic stem cells; MPP: multipotent progenitor; CMP: common myeloid progenitor; GMP: granulocyte-monocyte progenitor; MEP: megakaryocyte-erythroid progenitors.

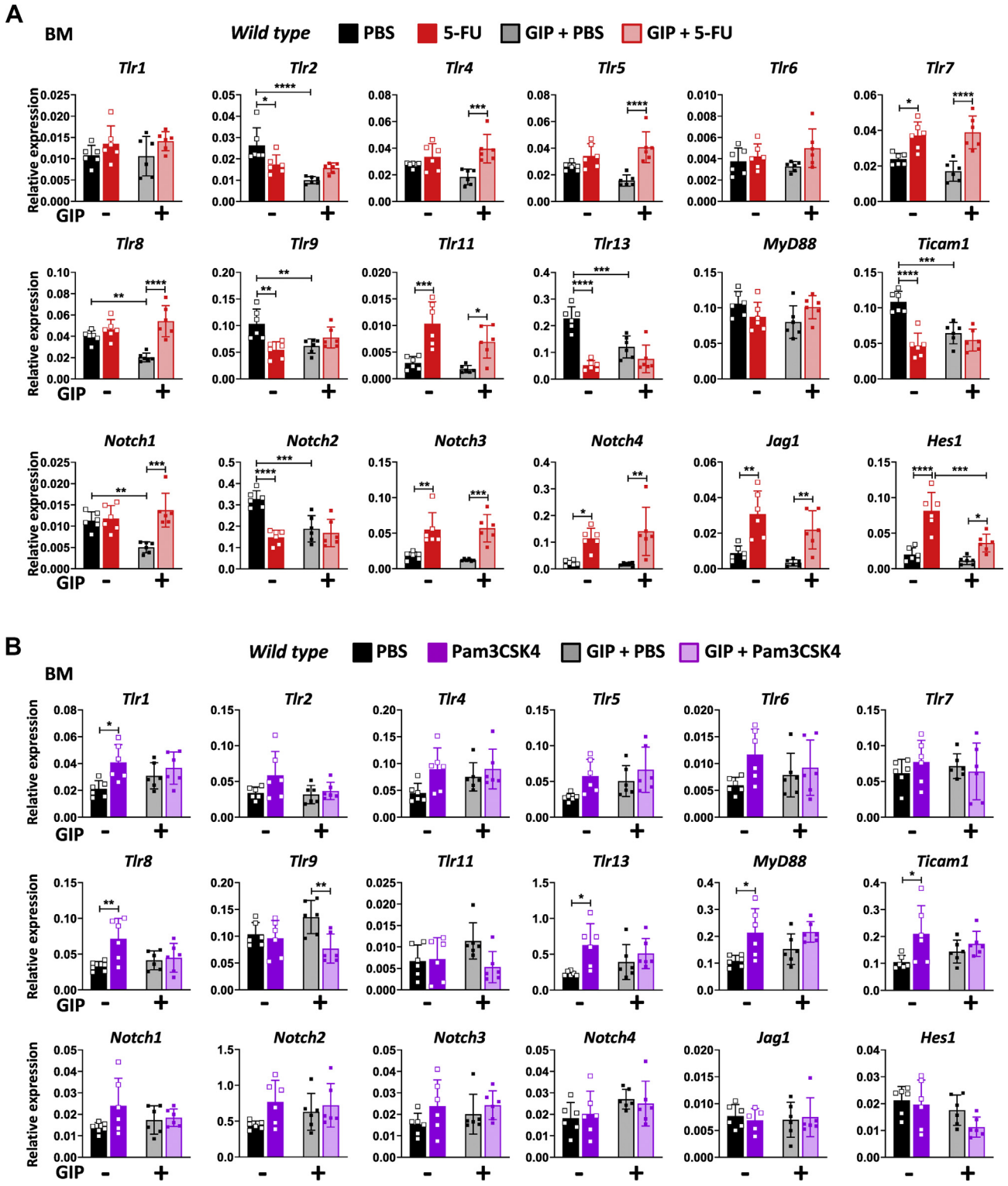

Figure 3: Bone marrow *Tlr* and *Notch* gene expression in response to 5-FU or Pam3CSK4 and [DAla2]-GIP coadministration. mRNA levels of the indicated TLR- and Notch-related genes, relative to *Ppia* gene expression, in bone marrow from 7-week-old WT male mice treated with PBS or [DAla2]-GIP and/or 5-FU (A) or Pam3CSK4 (B) as indicated (n = 6/group). Data are presented as the mean ± SD. $^{*}P \leq 0.05$, $^{**}P \leq 0.01$, $^{***}P \leq 0.001$, and $^{****}P \leq 0.0001$. 5-FU: 5-fluorouracil; Pam3CSK4: Pam3CysSerLys4; PBS: phosphate-buffered saline; GIP: glucose-dependent insulinotropic polypeptide; BM: bone marrow.

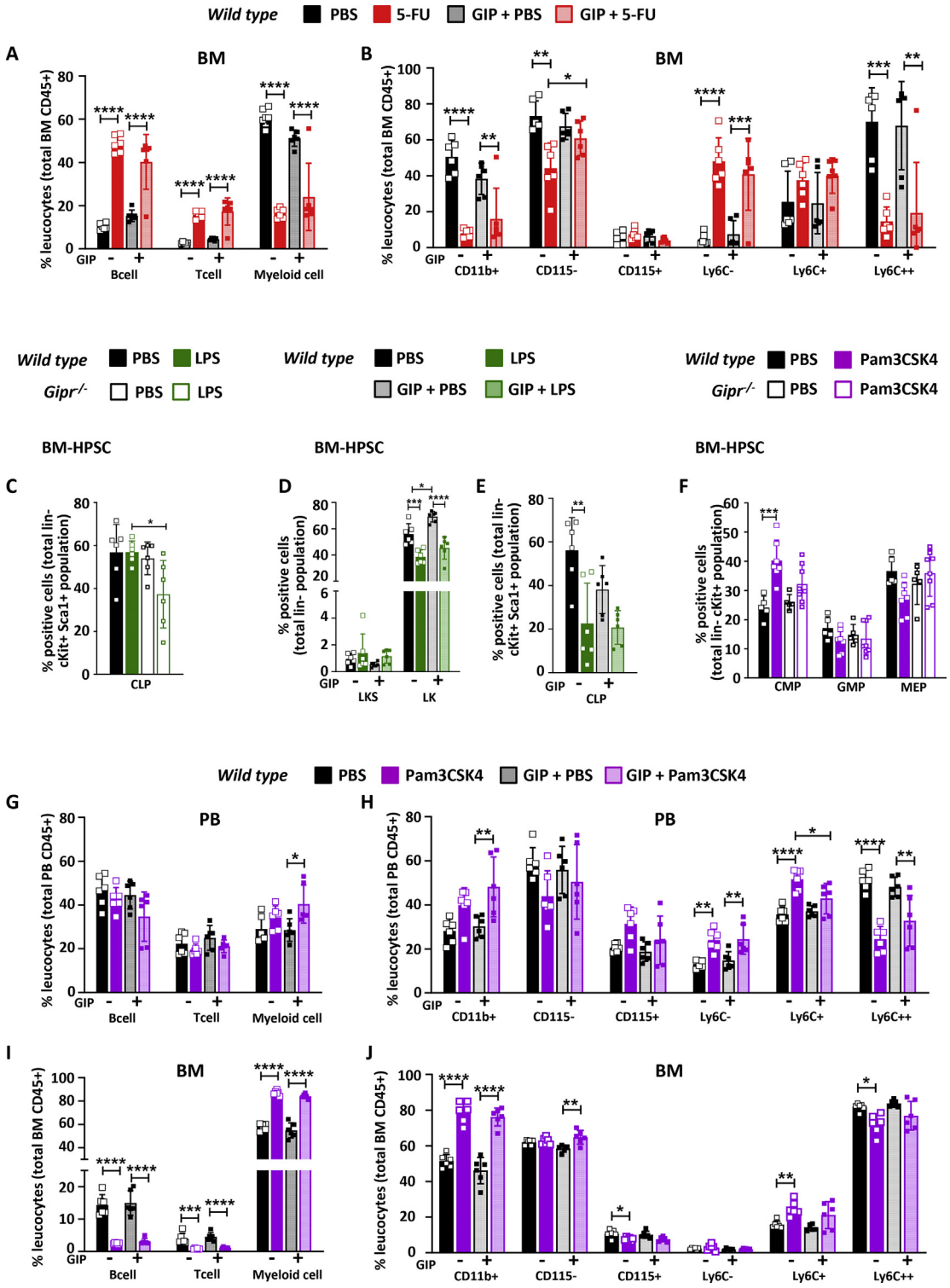

Figure 4: Hematopoietic responses to 5-FU, LPS, and Pam3CSK4 in *Gipr*$^{-/-}$ mice and WT mice treated with [DAla2]-GIP. Frequencies of B cells, T cells, M cells (A), and monocyte lineage cells (neutrophils and monocytes) (B) in bone marrow from 7-week-old WT males treated with [D-Ala]-GIP and/or 5-FU and controls (n = 6–8/group). (C) Frequency of CLP cells in bone marrow from 7-week-old WT and *Gipr*$^{-/-}$ male mice that were treated with LPS or vehicle (PBS) (n = 6/group). Frequency of LKS and LK populations (D) and CLP (E) cells in bone marrow from 7-week-old WT male mice treated with [D-Ala]-GIP and/or LPS and controls (n = 6/group). (F) Frequency of CMP, GMP, and MEP cells in bone marrow from 7-week-old WT and *Gipr*$^{-/-}$ male mice that were treated with Pam3CSK4 or vehicle (PBS) (n = 6/group). Frequencies of B cells, T cells, M cells, and monocyte lineage cells (neutrophils and monocytes) in peripheral blood (G, H) and bone marrow (I, J) from 7-week-old WT males treated with [D-Ala]-GIP and/or Pam3CSK4 and controls (n = 6/group). Data are presented as the mean ± SD. *$P \leq 0.05$, **$P \leq 0.01$, ***$P \leq 0.001$, and ****$P \leq 0.0001$. PBS: phosphate-buffered saline; 5-FU: 5-fluorouracil; LPS: Lipopolysaccharide; Pam3CSK4: Pam3CysSerLys4; GIP: glucose-dependent insulinotropic polypeptide; PB: peripheral blood; BM: bone marrow; BM-HPSC: bone marrow hematopoietic progenitor stem cells; LK: Lin-cKit + Sca1-; LKS: Lin-cKit + Sca1+; CLP: common lymphoid progenitor; CMP: common myeloid progenitor; GMP: granulocyte-monocyte progenitor; MEP: megakaryocyte-erythroid progenitors.

3.7. Modulation of GIPR signaling does not impair the hematopoietic response to LPS or Pam3CSK4

To determine the hematopoietic response to TLR engagement, we treated WT and *Gipr*$^{-/-}$ mice with the TLR ligands LPS or Pam3CSK4. Body weight was modestly lower in *Gipr*$^{-/-}$ mice treated with LPS, but not different in WT animals (Figures S9A-S9B). Spleen weight and splenic and femur cellularity were not different between genotypes (Figures S9C—S9F). LPS increased the frequency of myeloid populations in peripheral blood (Figure S9G), spleen (Figure S9H), and bone marrow (Figure S9I). In contrast, lymphoid cells (both B and T cells) were decreased in all tissues, except in the spleen where only T cells were reduced (Figures S9G—S9I). No differences in the response to LPS were detected between genotypes. Similarly, Lin-, LK, or LKS cell populations were not different (Figures S9J-S9K). The numbers of LT-ST HSCs were reduced, whereas MPPs were increased after LPS, to a similar extent in WT versus *Gipr*$^{-/-}$ mice (Figure S9L). Intriguingly, CLP populations were reduced by LPS only in the absence of the *Gipr* (Figure 4C), whereas proportions of CMPs, GMPs, and MEPs were not different in LPS-treated WT versus *Gipr*$^{-/-}$ mice (Figure S9M).

We next examined whether the activation of the GIPR impacted the hematopoietic response to LPS administration (Figure S10A). Body weight was reduced after LPS treatment and lower with [DAla2]-GIP administration (Figure S10B). No differences in spleen or femur weights or femur length were observed in [DAla2]-GIP-treated mice (Figures S10C—S10E). Femur cellularity was reduced in WT mice treated with [DAla2]-GIP alone (Figure S10F). Similarly, T cells, B cell, myeloid cell, neutrophil (CD115-), and monocyte (CD115+) cell populations in peripheral blood or BM were not different in [DAla2]-GIP-treated mice exposed to LPS (Figures S10G—S10J). [DAla2]-GIP administration increased LK cell proportions in BM (Figure 4D), while reducing CLP population (Figure 4E), without affecting other progenitor cell populations (Figures S10K—S10M).

Treatment with the TLR1/2 agonist Pam3CSK4 (Figure S11A) revealed no genotype-dependent differences in body weight, spleen, and femur weights, or femur and splenic cellularity (Figures S11B—S11F). Spleen weight was increased in Pam3CSK4-treated WT and *Gipr*$^{-/-}$ mice (Figure S11C); however, the numbers of B cells, T cells, and myeloid cells were not different in Pam3CSK4-treated WT versus *Gipr*$^{-/-}$ mice (Figures S11G—S11I). Myeloid cell populations were increased by Pam3CSK4 in peripheral blood, spleen and BM, without differences between genotypes (Figure S11G—I). Pam3CSK4 reduced B cell numbers in peripheral blood and BM, and T cell numbers in spleen and bone marrow (Figure S11G—I), however, no differences were observed between WT and *Gipr*$^{-/-}$ mice. Pam3CSK4 had a minimal genotype-dependent effect on BM-HPSC cell populations (Figure 4F, Figure S11J—S11M), with no differences being observed between WT and *Gipr*$^{-/-}$ mice. Similarly, the proportions of total lineage-negative populations were not different, LT-ST HSCs were decreased, and MPP frequencies were increased in both genotypes following Pam3CSK4 treatment (Figure S11J—L). CLP populations were similar (Figure S11M), however, CMP frequencies were increased in Pam3CSK4-treated WT but not *Gipr*$^{-/-}$ mice (Figure 4F). No genotype-dependent differences were observed in GMP and MEP progenitor cell populations (Figure 4F).

Coadministration of [DAla2]-GIP and Pam3CSK4 (Figure S12A) produced no differences in body weight (Figure S12B), spleen or femur weights, or femur cellularity compared to Pam3CSK4 alone (Figures S12C—S12F). B cell and T cell numbers were not different; however, myeloid cell numbers were higher in peripheral blood from mice treated with Pam3CSK4 plus [DAla2]-GIP versus [DAla2]-GIP alone (Figure 4G). CD11b + cells were increased with [DAla2]-GIP and Pam3CSK4 cotreatment, but the numbers of neutrophils (CD115-) and monocytes (CD115+) were not different (Figure 4H). [DAla2]-GIP treatment attenuated the induction of the inflammatory monocyte cell population (Ly6C+) by Pam3CSK4 (Figure 4H). BM T cells and B lymphocytes were reduced, whereas myeloid cells were increased by Pam3CSK4, without any impact of [DAla2]-GIP administration (Figure 4I). Interestingly, neutrophil levels (CD115-) were modestly increased in mice receiving [DAla2]-GIP and Pam3CSK4 versus mice treated with Pam3CSK4 alone (Figure 4J). No differences in Lin-cells, LKS, LK, LT-ST HSCs, MPPs, CLP, CMP, GMP, or MEPs were detected in the BM following [DAla2]-GIP administration in Pam3CSK4-treated mice (Figures S12G—S12K).

3.8. *Gipr*$^{-/-}$ BMT recipients are protected from HFD-induced adipose tissue inflammation

As GIPR + myeloid cells contribute to the control of WAT inflammation [38], we assessed mRNA transcripts relevant to inflammation in different WAT depots from *Gipr*$^{-/-}$ BM recipients fed an RCD or HFD for 16 weeks after BMT. In eWAT, the levels of *S100a8* and *S100a9* alarmin mRNA transcripts were increased after HFD feeding in WT but not in *Gipr*$^{-/-}$ BM-transplant recipients (Figure 5A). Similarly, *S100a8*, but not *S100a9*, was differentially expressed in iWAT of *Gipr*$^{-/-}$ BM-transplanted recipient mice (Figure 5B). Moreover, the HFD induction of *Il1b*, *Il6*, *Tnf*, *Ccl2*, *Adgrel* (F4/80), and *Cxcl2* mRNA expression in eWAT of WT BM recipients was markedly attenuated in mice receiving *Gipr*$^{-/-}$ BM (Figure 5A). Conversely, *Cxcl2* expression in iWAT was increased by HFD feeding only in *Gipr*$^{-/-}$ BM-transplanted mice (Figure 5B). Interestingly, the levels of *S100a9* and *Il6* in mWAT were increased in the recipients of *Gipr*$^{-/-}$ BM under RCD, but not HFD feeding (Figure S13A).

The analysis of eWAT from HFD-fed *Gipr*$^{-/-}$ mice revealed a reduction in *Tnf*, *Adgrel*, *Mgl2*, and *Cxcl1* gene expression, while only *Mgl2* was reduced in iWAT (Figures S13B-S13C). An increase in alarmin *S100a9* was observed in eWAT from *Gipr*$^{-/-}$ animals, whereas *Il1b* and *Tnf* mRNAs were increased in iWAT. In contrast, the levels of mRNA transcripts for *Il6*, *Ccl2*, *Adgrel*, and *Cxcl1* were reduced in *Gipr*$^{-/-}$ mWAT (Figure S13D). Taken together, these results reveal depot-specific differences in the contribution of BM-derived cells to HFD-associated changes in adipose tissue inflammation.

4. DISCUSSION

The availability of nutrients is a key determinant of hematopoiesis. Nutrient depletion or starvation reduces monocyte BM mobilization [39], enhances migration of memory T cells from peripheral organs to the BM [40], and shifts B cells from Peyer's patches to the BM, actions that are reversed upon refeeding [41]. Conversely, energy excess, as evident in mice exposed to an HFD, impairs hematopoiesis via reduction of BM HSPCs [42] or altered myelopoiesis, depending on the specific experimental context [43]. Although signals conveying nutrient status to BM populations are poorly understood, roles for leptin, 5′ AMP-activated protein kinase, CD36, and TLR4 as nutrient-sensitive regulators of hematopoiesis and adipose tissue inflammation have been proposed [44—47]. Here, we extend these concepts by highlighting new roles for the nutrient-sensitive GIP-GIPR axis in the control of hematopoiesis.

Previous studies have shown that HSCs from HFD-fed mice increase the number of proinflammatory macrophages in adipose tissue, via a hematopoietic MyD88-dependent process [48]. Moreover, experimental and clinical obesity has been linked to the dysregulation of hematopoiesis [42,47,48], mediated in part via gut-derived

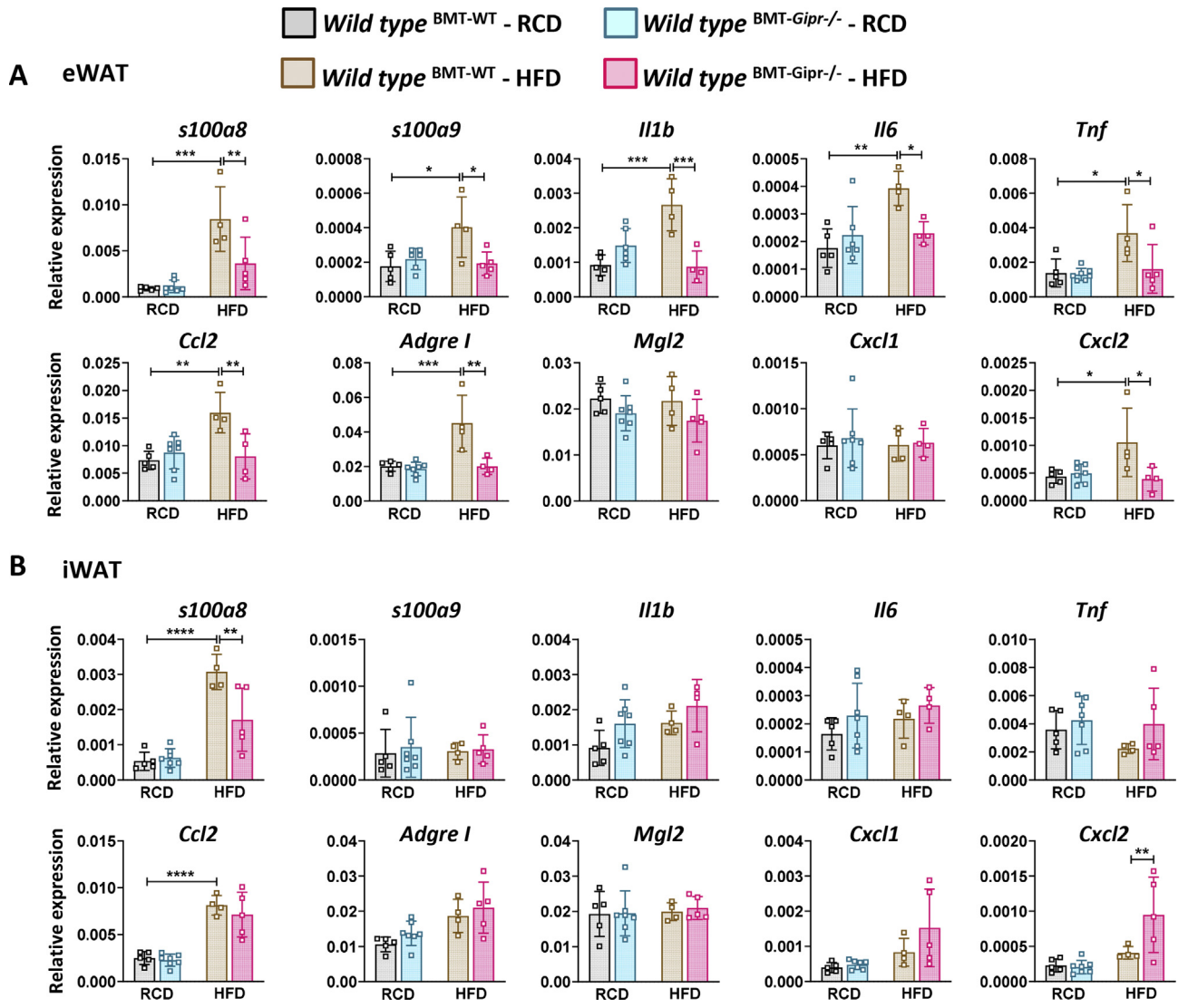

Figure 5: Modification of adipose tissue inflammation in HFD-fed mice after transplantation of *Gipr*$^{-/-}$ BM. Tissue mRNA expression of *S100a8*, *S100a9*, cytokines, and chemokines in eWAT (A) and iWAT (B) from 26-week-old WT male mice that received WT (BMT-WT) or *Gipr*$^{-/-}$ (BMT-*Gipr*$^{-/-}$) bone marrow at the age of 9 weeks and were fed an RCD (n = 4–7/group) or HFD (n = 4–5/group) for 12 weeks. Data are presented as the mean ± SD. *$P \leq 0.05$, **$P \leq 0.01$, ***$P \leq 0.001$, and ****$P \leq 0.0001$. BMT: bone marrow transplant; RCD: regular chow diet; HFD: high-fat diet; eWAT: epididymal white adipose tissue; iWAT: inguinal white adipose tissue.

mechanisms including nutrient signaling via fatty acids, as well as microbial-derived metabolites and TLR ligands [49,50]. In turn, BM TLR signaling regulates the extent of obesity-associated insulin resistance [46,51]. As circulating GIP levels are upregulated in the context of high-fat feeding, as well as experimental and clinical obesity [1,52–54], we hypothesized that GIPR signaling links energy availability to the control of hematopoiesis.

In this study, we showed that the absence of the GIPR in young healthy animals does not translate to a dysregulation of TLR or Notch gene expression within BM cells or any differences in hematopoiesis. In contrast, BM from older *Gipr*$^{-/-}$ mice fed an energy-rich diet displayed reduced expression of genes important for the TLR and Notch signaling pathways (Figure 6). Intriguingly, when BM cells were stressed using 5-FU or TLR agonists (LPS or Pam3CSK4), no differences in the expression of TLR- and Notch-related genes in *Gipr*$^{-/-}$ BM cells were observed. However, the activation of GIPR signaling in the context of concomitant 5-FU or Pam3CSK4 administration modified the expression of different TLR and Notch signaling members.

Gipr expression was localized to myeloid progenitors and within subsets of differentiated myeloid cells in the BM. Moreover, a marked reduction of *Gipr* mRNA within these cell lineages was observed within the BM of 8-week-old *Gipr*$^{Tie2-/-}$ mice. Nevertheless, the loss of GIPR within Tie2+ cells or globally within all tissues of *Gipr*$^{-/-}$ mice did not result in alteration of progenitor or differentiated lymphoid or myeloid cell populations in circulating blood, BM, or spleen. Hence, our current data do not support a critical role for Tie2-GIPR + cells in the basal control of hematopoiesis.

Similarly, we did not detect dysregulation of TLR or Notch gene expression in the BM of *Gipr*$^{Tie2-/-}$ mice, despite the marked reduction of *Gipr* expression within total BM RNA and in major *Gipr* + cell lineages within the BM. These results imply that signals arising from one or more GIPR + cell types not directly targeted by *Tie2-cre* contribute to the dysregulation of *Tlr* and *Notch* expression

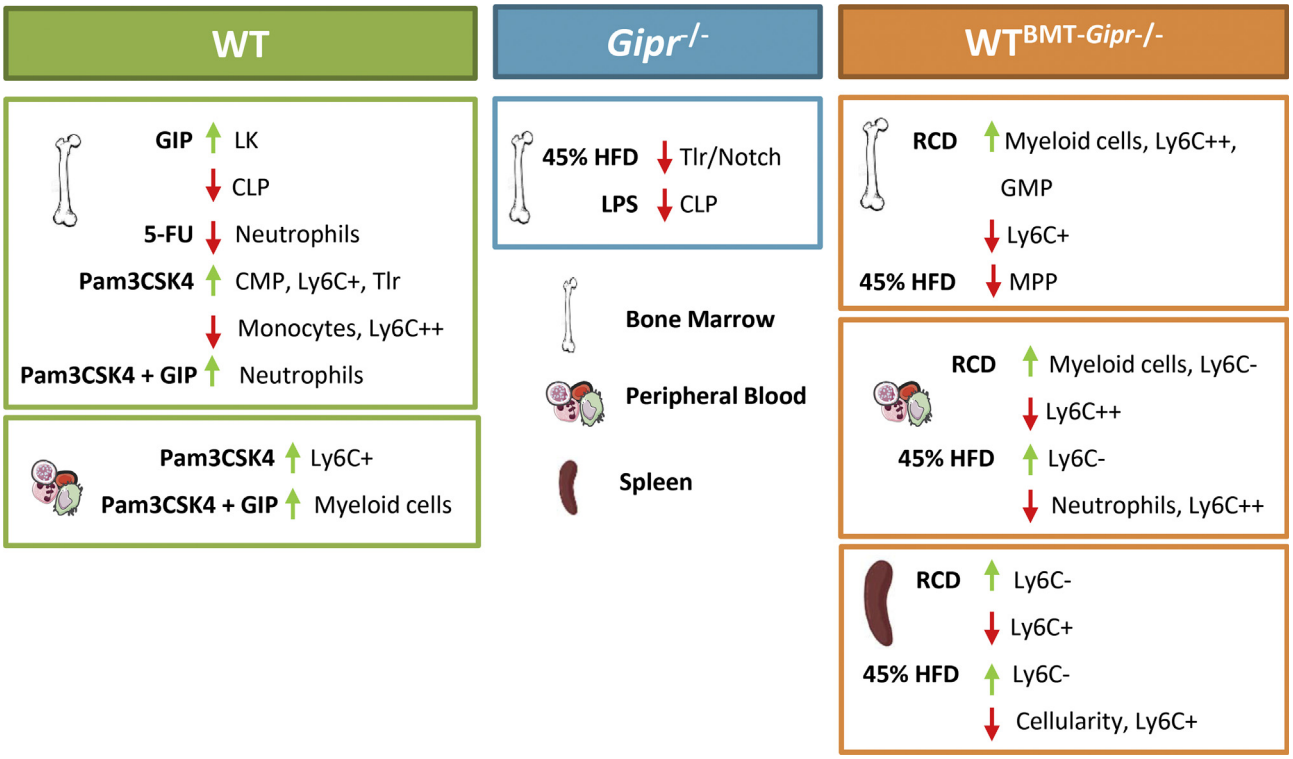

Figure 6: Gain and loss of GIPR signaling impact hematopoiesis. Bone marrow, peripheral blood, and splenic cells were assessed to investigate the role of the GIPR in the control of hematopoiesis in different stress situations. HFD: high-fat diet; RCD: regular chow diet; BMT: bone marrow transplant; 5-FU: 5-fluorouracil; LPS: Lipopolysaccharide; Pam3CSK4 = Pam3CysSerLys4; GIP: glucose-dependent insulinotropic polypeptide; LK: Lin-cKit + Sca1-; MPP: multipotent progenitor; CLP: common lymphoid progenitor; CMP: common myeloid progenitor; GMP: granulocyte-monocyte progenitor.

evident in *Gipr*$^{-/-}$ mice. Although developmental adaptation to germline deletion of *Gipr* may contribute to these different observations, the reduced expression of a subset of these genes in the BM of mice transplanted with *Gipr*$^{-/-}$ BM demonstrates that these findings reflect a BM-intrinsic process. Hence, it seems unlikely that the compensation for developmental loss of *Gipr* expression underlies sustained dysregulation of BM *Tlr* and *Notch* expression following the loss of the *Gipr*.

The reduced expression of TLR and Notch family members raised the possibility that *Gipr*$^{-/-}$ mice might exhibit defective mobilization of hematopoietic cells in response to TLR ligands. Nevertheless, we did not detect major differences in the acute hematopoietic responses to the TLR agonists LPS or Pam3CSK4. Intriguingly, the representation of the CLP population was reduced following the LPS administration in *Gipr*$^{-/-}$ mice, raising the possibility that the loss of the GIPR differentially impacts the biology of the lymphoid differentiating cells, findings which merit further exploration.

Interestingly, we detected reduced eWAT expression of the alarmins *S100a8* and *S100a9*, as well as attenuated WAT expression of genes encoding cytokines, chemokines, and F4/80, a marker of macrophage infiltration, following selective deletion of the GIPR within the BM. Hence, these findings, taken together with our recent studies [20,38], add further support for the BM GIPR as a determinant of the extent of adipose tissue inflammation in the context of nutrient excess.

Of potential translational relevance, exogenous GIPR agonism had no major deleterious consequences on the BM hematopoietic responses to experimental stressors such as 5-FU, LPS, or Pam3CSK4. Interestingly, circulating myeloid numbers were higher in [DAla2]-GIP-treated mice after Pam3CSK4. As a complementary approach to identify the functional importance of BM GIPR + cell populations, we used noncompetitive BM repopulation to examine cell lineages within the BM and peripheral blood. A reduction in circulating and splenic monocyte cell populations was evident as early as 4 weeks after the transplantation in *Gipr*$^{-/-}$ BM recipients. Although RCD-fed *Gipr*$^{-/-}$ BM recipients showed a decrease in circulating proinflammatory monocytes (Ly6C^{++}), this same population was increased in isolated BM cells, accompanied by a decrease in monocytes (LyC6^{+}). Similarly, HFD-fed *Gipr*$^{-/-}$ BM recipient mice had a decrease in circulating proinflammatory monocytes (Ly6C^{++}) and neutrophils (CD115^{-}) compared to WT BM-transplanted mice. Taken together with the dysregulated expression of inflammatory genes within adipose tissue, the transplantation experiments illustrate an important biological role of the BM GIPR in the formation of hematopoietic lineages and the response to HFD feeding (Figure 6).

Our studies have several limitations. First, several analyses used mice with germline inactivation of the *Gipr* gene, and hence developmental adaptations may have masked the importance of the loss of the GIPR in the hematopoietic system of adult mice. Although *Gipr* expression has been difficult to detect in normal endothelial cells [33] and was not reduced within major blood vessels of *Gipr*$^{Tie2-/-}$ mice, it remains possible that low-level *Gipr* expression within subsets of endothelial cells, when extinguished, may contribute to the phenotypes observed. Moreover, BMT may confer partial resistance to diet-induced obesity [55], potentially attenuating metabolic phenotypes arising in recipients of *Gipr*$^{-/-}$ BM. We did not study the importance of the GIPR for hematopoiesis in markedly obese older mice with severe insulin resistance, metabolic features likely to be found in human populations targeted therapeutically for

manipulation of the GIPR signaling system. Similarly, it will be interesting to assess the importance of the GIPR for hematopoiesis under conditions characterized by bacterial and viral infections, cancer, and additional immune challenges, which may unmask new roles for the hematopoietic GIPR in these contexts. Additionally, we analyzed the gene expression in RNA from the whole BM and adipose tissue, potentially obscuring meaningful changes in cellular subsets within the tissue microenvironment.

Our current findings reveal that the gain and loss of GIPR signaling produce dysregulation of hematopoiesis and myeloid lineages and regulate the expression of multiple BM TLR and Notch genes (Figure 6), as well as the control of adipose tissue inflammation. Collectively, these observations are consistent with a role for GIP as a gut-derived signal communicating changes in nutrient intake to the BM compartment. However, our analyses do not support an important role for the GIPR in the control of basal or adaptive hematopoiesis. As GIP-based coagonists such as tirzepatide [5,56] are in phase 3 clinical trials and GIPR antagonism continues to be explored therapeutically [6,7,13], our findings support the hematopoietic safety of translational studies targeting the GIPR for the treatment of metabolic disorders.

AUTHORS' CONTRIBUTIONS

Conceptualization was contributed by G. P., and D. J. D.; investigation, G. P., E. M. V., L. L. B., E. E. M., J. A. K., D. M., and K. W. A. B.; formal analysis and visualization, G. P.; writing the original draft, G. P. D. J. D; reviewing and editing the manuscript, G. P., E. M. V., L. L. B., E. E. M., J. A. K., and D. J. D.; funding acquisition and project administration, D. J. D.; supervision, D. J. D. In addition, D. J. D. takes the primary responsibility for the data described in this manuscript.

ACKNOWLEDGMENTS

G. P. has received a postdoctoral fellowship from the Institut d'Investigacions Biomèdiques August Pi i Sunyer (IDIBAPS). E. M. V. received fellowship funding from Diabetes Canada. E. E. M. has received fellowship funding from the Canadian Diabetes Association and the Canadian Institutes of Health Research. D. J. D. was supported by a CIHR Foundation Grant 154321, an investigator-initiated operating grant from Novo Nordisk Inc., the Novo Nordisk Foundation-Sinai Health-University of Toronto Fund in Incretin biology, the Canada-Israel Health Research Initiative, jointly funded by the Canadian Institutes of Health Research 154321, the Israel Science Foundation, the International Development Research Centre, and the Azrieli Foundation, and a Banting and Best Diabetes Centre-Novo Nordisk Chair in Incretin biology. Some of the equipment used in this study was supported by the 3D (Diet, Digestive Tract, and Disease) Centre funded by the Canadian Foundation for Innovation and Ontario Research Fund, project numbers 19442 and 30961. We thank J. E. Dick, S. Xie, and J. F. Woolley for their scientific guidance and assistance.

CONFLICT OF INTEREST

D. J. D. has served as an advisor or consultant or speaker within the past 12 months to Forkhead Biotherapeutics, Intarcia Therapeutics, Merck Research Laboratories, Novo Nordisk Inc., and Pfizer Inc. None of the other authors has conflicts of interest. Investigator-initiated research for studies of GLP-1 and GIP is supported in part by grants from Novo Nordisk Inc. To Mt. Sinai Hospital and D. J. D.

APPENDIX A. SUPPLEMENTARY DATA

Supplementary data to this article can be found online at https://doi.org/10.1016/j.molmet.2020.101008.

REFERENCES

[1] Campbell, J.E., Drucker, D.J., 2013. Pharmacology physiology and mechanisms of incretin hormone action. Cell Metabolism 17(4):819—837.

[2] Muller, T.D., Finan, B., Bloom, S.R., D'Alessio, D., Drucker, D.J., Flatt, P.R., et al., 2019. Glucagon-like peptide 1 (GLP-1). Mol Metab, 3072—3130.

[3] Drucker, D.J., 2016. The cardiovascular biology of glucagon-like peptide-1. Cell Metabolism 24(1):15—30.

[4] Nauck, M.A., Meier, J.J., Cavender, M.A., Abd El Aziz, M., Drucker, D.J., 2017. Cardiovascular actions and clinical outcomes with glucagon-like peptide-1 receptor agonists and dipeptidyl peptidase-4 inhibitors. Circulation 136(9): 849—870.

[5] Frias, J.P., Nauck, M.A., Van, J., Kutner, M.E., Cui, X., Benson, C., et al., 2018. Efficacy and safety of LY3298176, a novel dual GIP and GLP-1 receptor agonist, in patients with type 2 diabetes: a randomised, placebo-controlled and active comparator-controlled phase 2 trial. Lancet 392(10160):2180—2193.

[6] Finan, B., Muller, T.D., Clemmensen, C., Perez-Tilve, D., DiMarchi, R.D., Tschop, M.H., 2016. Reappraisal of GIP pharmacology for metabolic diseases. Trends in Molecular Medicine 22(5):359—376.

[7] Killion, E.A., Lu, S.C., Fort, M., Yamada, Y., Veniant, M.M., Lloyd, D.J., 2020. Glucose-dependent insulinotropic polypeptide receptor therapies for the treatment of obesity, do agonists = antagonists? Endocrine Reviews 41(1).

[8] Kaneko, K., Fu, Y., Lin, H.Y., Cordonier, E.L., Mo, Q., Gao, Y., et al., 2019. Gut-derived GIP activates central Rap1 to impair neural leptin sensitivity during overnutrition. Journal of Clinical Investigation, 1303786—1303791.

[9] Adriaenssens, A.E., Biggs, E.K., Darwish, T., Tadross, J., Sukthankar, T., Girish, M., et al., 2019. Glucose-dependent insulinotropic polypeptide receptor-expressing cells in the hypothalamus regulate food intake. Cell Metabolism 30(5):987—996 e986.

[10] Campbell, J.E., Ussher, J.R., Mulvihill, E.E., Kolic, J., Baggio, L.L., Cao, X., et al., 2016. TCF1 links GIPR signaling to the control of beta cell function and survival. Nature Medicine 2284—90.

[11] Thondam, S.K., Daousi, C., Wilding, J.P., Holst, J.J., Ameen, G.I., Yang, C., et al., 2017. Glucose-dependent insulinotropic polypeptide promotes lipid deposition in subcutaneous adipocytes in obese type 2 diabetes patients: a maladaptive response. American Journal of Physiology. Endocrinology and Metabolism 312(3):E224—E233.

[12] Miyawaki, K., Yamada, Y., Ban, N., Ihara, Y., Tsukiyama, K., Zhou, H., et al., 2002. Inhibition of gastric inhibitory polypeptide signaling prevents obesity. Nature Medicine 8(7):738—742.

[13] Killion, E.A., Wang, J., Yie, J., Shi, S.D., Bates, D., Min, X., et al., 2018. Anti-obesity effects of GIPR antagonists alone and in combination with GLP-1R agonists in preclinical models. Science Translational Medicine 10(472).

[14] Svendsen, B., Capozzi, M.E., Nui, J., Hannou, S.A., Finan, B., Naylor, J., et al., 2020. Pharmacological antagonism of the incretin system protects against diet-induced obesity. Mol Metab, 3244—3255.

[15] Zhong, Q., Itokawa, T., Sridhar, S., Ding, K.H., Xie, D., Kang, B., et al., 2007. Effects of glucose-dependent insulinotropic peptide on osteoclast function. American Journal of Physiology. Endocrinology and Metabolism 292(2):E543—E548.

[16] Bollag, R.J., Zhong, Q., Phillips, P., Min, L., Zhong, L., Cameron, R., et al., 2000. Osteoblast-derived cells express functional glucose-dependent insulinotropic peptide receptors. Endocrinology 141(3):1228—1235.

[17] Nagashima, M., Watanabe, T., Terasaki, M., Tomoyasu, M., Nohtomi, K., Kim-Kaneyama, J., et al., 2011. Native incretins prevent the development of atherosclerotic lesions in apolipoprotein E knockout mice. Diabetologia 54(10): 2649—2659.

[18] Nogi, Y., Nagashima, M., Terasaki, M., Nohtomi, K., Watanabe, T., Hirano, T., 2012. Glucose-dependent insulinotropic polypeptide prevents the progression

of macrophage-driven atherosclerosis in diabetic apolipoprotein E-null mice. PloS One 7(4):e35683.

[19] Pivovarova, O., Hornemann, S., Weimer, S., Lu, Y., Murahovschi, V., Zhuk, S., et al., 2015. Regulation of nutrition-associated receptors in blood monocytes of normal weight and obese humans. Peptides, 6512—6519.

[20] Mantelmacher, F.D., Fishman, S., Cohen, K., Pasmanik Chor, M., Yamada, Y., Zvibel, I., et al., 2017. Glucose-dependent insulinotropic polypeptide receptor deficiency leads to impaired bone marrow hematopoiesis. The Journal of Immunology 198(8):3089—3098.

[21] Nagai, Y., Garrett, K.P., Ohta, S., Bahrun, U., Kouro, T., Akira, S., et al., 2006. Toll-like receptors on hematopoietic progenitor cells stimulate innate immune system replenishment. Immunity 24(6):801—812.

[22] Sioud, M., Floisand, Y., Forfang, L., Lund-Johansen, F., 2006. Signaling through toll-like receptor 7/8 induces the differentiation of human bone marrow CD34+ progenitor cells along the myeloid lineage. Journal of Molecular Biology 364(5):945—954.

[23] Takizawa, H., Regoes, R.R., Boddupalli, C.S., Bonhoeffer, S., Manz, M.G., 2011. Dynamic variation in cycling of hematopoietic stem cells in steady state and inflammation. Journal of Experimental Medicine 208(2):273—284.

[24] Rodriguez, S., Chora, A., Goumnerov, B., Mumaw, C., Goebel, W.S., Fernandez, L., et al., 2009. Dysfunctional expansion of hematopoietic stem cells and block of myeloid differentiation in lethal sepsis. Blood 114(19):4064—4076.

[25] Esplin, B.L., Shimazu, T., Welner, R.S., Garrett, K.P., Nie, L., Zhang, Q., et al., 2011. Chronic exposure to a TLR ligand injures hematopoietic stem cells. The Journal of Immunology 186(9):5367—5375.

[26] Megias, J., Yanez, A., Moriano, S., O'Connor, J.E., Gozalbo, D., Gil, M.L., 2012. Direct Toll-like receptor-mediated stimulation of hematopoietic stem and progenitor cells occurs in vivo and promotes differentiation toward macrophages. Stem Cells 30(7):1486—1495.

[27] Miyawaki, K., Yamada, Y., Yano, H., Niwa, H., Ban, N., Ihara, Y., et al., 1999. Glucose intolerance caused by a defect in the entero-insular axis: a study in gastric inhibitory polypeptide receptor knockout mice. Proceedings of the National Academy of Sciences of the U S A 96(26):14843—14847.

[28] de Lange, W.J., Halabi, C.M., Beyer, A.M., Sigmund, C.D., 2008. Germ line activation of the Tie2 and SMMHC promoters causes noncell-specific deletion of floxed alleles. Physiological Genomics 35(1):1—4.

[29] Koehler, J.A., Baggio, L.L., Yusta, B., Longuet, C., Rowland, K.J., Cao, X., et al., 2015. GLP-1R agonists promote normal and neoplastic intestinal growth through mechanisms requiring Fgf7. Cell Metabolism 21(3):379—391.

[30] Mulvihill, E.E., Varin, E.M., Gladanac, B., Campbell, J.E., Ussher, J.R., Baggio, L.L., et al., 2017. Cellular sites and mechanisms linking reduction of dipeptidyl peptidase-4 activity to control of incretin hormone action and glucose homeostasis. Cell Metabolism 25(1):152—165.

[31] Pajcini, K.V., Speck, N.A., Pear, W.S., 2011. Notch signaling in mammalian hematopoietic stem cells. Leukemia 25(10):1525—1532.

[32] Tang, Y., Harrington, A., Yang, X., Friesel, R.E., Liaw, L., 2010. The contribution of the Tie2+ lineage to primitive and definitive hematopoietic cells. Genesis 48(9):563—567.

[33] Pujadas, G., Drucker, D.J., 2016. Vascular biology of glucagon receptor superfamily peptides: mechanistic and clinical relevance. Endocrine Reviews 37(6):554—583.

[34] Randall, T.D., Weissman, I.L., 1997. Phenotypic and functional changes induced at the clonal level in hematopoietic stem cells after 5-fluorouracil treatment. Blood 89(10):3596—3606.

[35] Herman, A.C., Monlish, D.A., Romine, M.P., Bhatt, S.T., Zippel, S., Schuettpelz, L.G., 2016. Systemic TLR2 agonist exposure regulates hematopoietic stem cells via cell-autonomous and cell-non-autonomous mechanisms. Blood Cancer Journal 6e437.

[36] Lamont, B.J., Drucker, D.J., 2008. Differential anti-diabetic efficacy of incretin agonists vs. DPP-4 inhibition in high fat fed mice. Diabetes 57(1):190—198.

[37] Ussher, J.R., Campbell, J.E., Mulvihill, E.E., Baggio, L.L., Bates, H.E., McLean, B.A., et al., 2018. Inactivation of the glucose-dependent insulinotropic polypeptide receptor improves outcomes following experimental myocardial infarction. Cell Metabolism 27(2):450—460.

[38] Mantelmacher, F.D., Zvibel, I., Cohen, K., Epshtein, A., Pasmanik-Chor, M., Vogl, T., et al., 2019. GIP regulates inflammation and body weight by restraining myeloid-cell-derived S100A8/A9. Nature Metabolism 1(1):58—69.

[39] Jordan, S., Tung, N., Casanova-Acebes, M., Chang, C., Cantoni, C., Zhang, D., et al., 2019. Dietary intake regulates the circulating inflammatory monocyte pool. Cell 178(5):1102—1114 e1117.

[40] Collins, N., Han, S.J., Enamorado, M., Link, V.M., Huang, B., Moseman, E.A., et al., 2019. The bone marrow protects and optimizes immunological memory during dietary restriction. Cell 178(5):1088—1101 e1015.

[41] Nagai, M., Noguchi, R., Takahashi, D., Morikawa, T., Koshida, K., Komiyama, S., et al., 2019. Fasting-refeeding impacts immune cell dynamics and mucosal immune responses. Cell 178(5):1072—1087 e1014.

[42] van den Berg, S.M., Seijkens, T.T., Kusters, P.J., Beckers, L., den Toom, M., Smeets, E., et al., 2016. Diet-induced obesity in mice diminishes hematopoietic stem and progenitor cells in the bone marrow. The FASEB Journal 30(5):1779—1788.

[43] Christ, A., Gunther, P., Lauterbach, M.A.R., Duewell, P., Biswas, D., Pelka, K., et al., 2018. Western diet triggers NLRP3-dependent innate immune reprogramming. Cell 172(1—2):162—175 e114.

[44] Galic, S., Fullerton, M.D., Schertzer, J.D., Sikkema, S., Marcinko, K., Walkley, C.R., et al., 2011. Hematopoietic AMPK beta1 reduces mouse adipose tissue macrophage inflammation and insulin resistance in obesity. Journal of Clinical Investigation 121(12):4903—4915.

[45] Nicholls, H.T., Kowalski, G., Kennedy, D.J., Risis, S., Zaffino, L.A., Watson, N., et al., 2011. Hematopoietic cell-restricted deletion of CD36 reduces high-fat diet-induced macrophage infiltration and improves insulin signaling in adipose tissue. Diabetes 60(4):1100—1110.

[46] Saberi, M., Woods, N.B., de Luca, C., Schenk, S., Lu, J.C., Bandyopadhyay, G., et al., 2009. Hematopoietic cell-specific deletion of toll-like receptor 4 ameliorates hepatic and adipose tissue insulin resistance in high-fat-fed mice. Cell Metabolism 10(5):419—429.

[47] Liu, A., Chen, M., Kumar, R., Stefanovic-Racic, M., O'Doherty, R.M., Ding, Y., et al., 2018. Bone marrow lympho-myeloid malfunction in obesity requires precursor cell-autonomous TLR4. Nature Communications 9(1):708.

[48] Singer, K., DelProposto, J., Morris, D.L., Zamarron, B., Mergian, T., Maley, N., et al., 2014. Diet-induced obesity promotes myelopoiesis in hematopoietic stem cells. Mol Metab 3(6):664—675.

[49] Yan, H., Baldridge, M.T., King, K.Y., 2018. Hematopoiesis and the bacterial microbiome. Blood 132(6):559—564.

[50] Griffin, C., Eter, L., Lanzetta, N., Abrishami, S., Varghese, M., McKernan, K., et al., 2018. TLR4, TRIF, and MyD88 are essential for myelopoiesis and CD11c(+) adipose tissue macrophage production in obese mice. Journal of Biological Chemistry 293(23):8775—8786.

[51] Razolli, D.S., Moraes, J.C., Morari, J., Moura, R.F., Vinolo, M.A., Velloso, L.A., 2015. TLR4 expression in bone marrow-derived cells is both necessary and sufficient to produce the insulin resistance phenotype in diet-induced obesity. Endocrinology 156(1):103—113.

[52] Creutzfeldt, W., Ebert, R., Willms, B., Frerichs, H., Brown, J.C., 1978. Gastric inhibitory polypeptide (GIP) and insulin in obesity: increased response to stimulation and defective feedback control of serum levels. Diabetologia 14(1):15—24.

[53] Salera, M., Giacomoni, P., Pironi, L., Cornia, G., Capelli, M., Marini, A., et al., 1982. Gastric inhibitory polypeptide release after oral glucose: relationship to glucose intolerance, diabetes mellitus, and obesity. Journal of Clinical Endocrinology & Metabolism 55(2):329—336.

[54] Hampton, S.M., Kwasowski, P., Tan, K., Morgan, L.M., Marks, V., 1983. Effect of pretreatment with a high fat diet on the gastric inhibitory polypeptide and insulin responses to oral triolein and glucose in rats. Diabetologia 24(4):278—281.

[55] Katiraei, S., Hoving, L.R., van Beek, L., Mohamedhoesein, S., Carlotti, F., van Diepen, J.A., et al., 2017. BMT decreases HFD-induced weight gain associated

with decreased preadipocyte number and insulin secretion. PloS One 12(4): e0175524.

[56] Frias, J.P., Nauck, M.A., Van, J., Benson, C., Bray, R., Cui, X., et al., 2020. Efficacy and tolerability of tirzepatide, a dual glucose-dependent insulinotropic peptide and glucagon-like peptide-1 receptor agonist in patients with type 2 diabetes: a 12-week, randomized, double-blind, placebo-controlled study to evaluate different dose-escalation regimens. Diabetes, Obesity and Metabolism.

